Supramolecular Chemistry
Publication details, including instructions for authors and subscription information:
http://www.informaworld.com/smpp/title~content=t713649759

Complexation with diol host compounds. Part 17. Structures and thermal analysis of 9,9'-dihydroxy-9,9'-bifluorene with ethanol, 1-butanol and pyridine

Leonard J. Barbour[a]; Mino R. Caira[a]; Luigi R. Nassimbeni[a]; Andreas Wierig[b]; Edwin Weber[b]
[a] Department of Chemistry, University of Cape Town, Rondebosch, South Africa [b] Institut für Organische Chemie, Technische Universität Bergakademie, Freiberg, Germany

To cite this Article Barbour, Leonard J. , Caira, Mino R. , Nassimbeni, Luigi R. , Wierig, Andreas and Weber, Edwin(1995) 'Complexation with diol host compounds. Part 17. Structures and thermal analysis of 9,9'-dihydroxy-9,9'-bifluorene with ethanol, 1-butanol and pyridine', Supramolecular Chemistry, 5: 2, 153 — 158

To link to this Article: DOI: 10.1080/10610279508029488

URL: http://dx.doi.org/10.1080/10610279508029488

SUPRAMOLECULAR CHEMISTRY, Vol. 5, pp. 153–158
Reprints available directly from the publisher
Photocopying permitted by license only

Complexation with diol host compounds. Part 17. Structures and thermal analysis of 9,9'-dihydroxy-9,9'-bifluorene with ethanol, 1-butanol and pyridine

LEONARD J. BARBOUR[a], MINO R. CAIRA[a], LUIGI R. NASSIMBENI[a]*, ANDREAS WIERIG[b] and EDWIN WEBER[b]*

[a]Department of Chemistry, University of Cape Town, Rondebosch 7700, South Africa and [b]Institut für Organische Chemie, Technische Universität Bergakademie, Leipziger Strasse 29, D-09596 Freiberg, Germany

(Received June 15, 1994)

Structures of the inclusion compound 9,9'-dihydroxy-9,9'-bifluorene with ethanol, 1-butanol and pyridine have been determined. The structures are stabilised by networks of hydrogen bonds. The thermal analysis indicates a single step decomposition process with concomitant phase transition of the structures. Accurate vapour pressure measurements at various temperatures yield the enthalpy change for the guest release reaction.

Weber has recently reviewed the principles of directed host design,[1] and has shown that a successful host molecule should be bulky and rigid, in order to provide suitable cavities in the crystal structure. Moreover, it is often helpful to have a high affinity functional group in the molecule which will be engaged in specific host-guest interactions.

We have studied a variety of inclusion compounds where the host molecules contain the hydroxyl moiety as hydrogen-bonding donor, shielded by bulky groups which yield suitable spaces which can accommodate selected guest molecules. Thus we have elucidated the crystal structures of the inclusion compounds of *trans*-9,10-dihydroxy-9,10-diphenyl-9,10-dihydroanthracene with various ketones[2,3] and substituted pyridines.[4] We have also studied a series of 'wheel-and-axle' host compounds such as 1,1,2,2-tetraphenylethane-1,2-diol, and demonstrated its ability to discriminate between lutidine isomers,[5] and we have measured the thermal stabilities of several inclusion compounds of 1,1,6,6-tetraphenyl-2,4-diyne-1,6-diol with the xylenes.[6] Host compounds which contain the fluorenyl moiety have proved to be particularly versatile[7] and we now present the structural and thermal stability results of the inclusion compounds formed between the host 9,9'-dihydroxy-9,9'-bifluorene (**1**) and ethanol, 1-butanol and pyridine (**2**–**4**).

EXPERIMENTAL

Synthesis

The host compound **1** was synthesised by reaction of solutions of magnesium iodide (prepared from iodine and magnesium turnings) in dried benzene-Et_2O and fluorenone in hot benzene. Workup including hydrolysis with H_2O, collection of the precipitate, treatment with hot EtOH and recrystallisation from MeOH yielded a white powder (85%), m.p. 190°C (lit.,[8] 190–192°C).

Crystal Structure Determination

Single crystals of the inclusion compounds **2**–**4** suitable for X-ray diffraction were obtained by slow evaporation over a period of 10 days. Preliminary cell dimensions

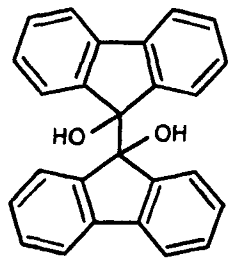

2 = **1**•EtOH (2:1)
3 = **1**•Bu^nOH (2:1)
4 = **1**•Pyridine (1:1)

Scheme 1

---

*To whom correspondence should be addressed.

and space group symmetry were determined photographically. X-ray diffraction data were then measured on an Envaf-Nonius. CAD4 diffractometer using graphite-monochromated MoK_α radiation and the ω-2θ scan mode. Measurements were carried out at 293K and crystal stabilities were checked by monitoring three reference reflections periodically. Crystal data are given in Table 1. All data were corrected for Lorentz and polarisation effects, but not for absorption.

The structures were solved by direct methods using SHELX-86 and refined using the SHELX-76 program system. For **2** all the heavy atoms of the host molecule were treated anisotropically and the aromatic hydrogens were refined in geometrically constrained positions with a common isotropic temperature factor. Only one hydroxyl hydrogen could be successfully located and was finally refined with the O-H distance constrained to 0.97Å. The ethanol atoms displayed high thermal motion and the final refinement of the guest employed geometric constraints and isotropic temperature factors. No attempt was made to refine the guest hydrogens. Compounds **3** and **4** were refined similarly, except that the positions of the guest molecules were better defined and allowed us to refine them with anisotropic temperature factors and with guest hydrogens in constrained positions. Final positional atomic coordinates, anisotropic thermal parameters, bond lengths, bond angles and tables of structure factors have been deposited. The atomic numbering scheme is shown in Fig. 1 which shows a typical molecular conformation of a host molecule.

Thermal Analysis

Thermogravimetry (TG) and differential scanning calorimetry (DSC) were performed on a Perkin Elmer PC7 series system. Crystals were removed from their mother liquor, blotted dry on filter paper, and crushed. Sample weight in each case was ca 5 mg, the heating rate was 10 Kmin^{-1}, and the samples were purged by a stream of nitrogen flowing at 40 cm^{3}min^{-1}.

RESULTS AND DISCUSSION

The crystallographic asymmetric unit in **2** comprises two host molecules and a guest ethanol, all interlinked by hydrogen bonds as shown in Fig. 2. The conformation of a

Table 1 Crystal data, data collection and final refinement parameters

CRYSTAL DATA			
Compound	**2**	**3**	**4**
Guest	Ethanol	n-Butanol	Pyridine
Molecular formula	$2(C_{26}H_{18}O_2)•C_2H_6O$	$2(C_{26}H_{18}O_2)•C_4H_{10}O$	$C_{26}H_{18}O_2•C_5H_5N$
M_r	770.92	798.98	441.53
Space group	$P\bar{1}$	$P\bar{1}$	P2/n
Z	2	2	8
a (Å)	10.639(11)	12.911(2)	20.439(15)
b (Å)	14.058(6)	13.262(1)	9.199(1)
c (Å)	14.608(12)	13.287(1)	27.060(1)
α (°)	71.64(5)	93.57(1)	90
β (°)	74.27(9)	111.57(1)	108.94(6)
γ (°)	88.57(7)	95.15(1)	90
Volume (Å^3)	1992(3)	2096.9(4)	4812(5)
D_m (gcm^{-3})	1.28(1)	1.26(1)	1.22(1)
D_c (gcm^{-3})	1.285	1.265	1.219
μ (Mo K_α) (cm^{-1})	0.75	0.74	0.71
F(000)	812	844	1856
DATA COLLECTION PARAMETERS			
Crystal dimensions (mm)	0.41 × 0.41 × 0.47	0.47 × 0.47 × 0.44	0.28 × 0.31 × 0.38
θ range scanned (°)	1–23	1–23	1–23
Range of indices *h,k,l*	±11,±15,16	±14,±14,14	±22,10,29
Total exposure time (hrs)	41.0	37.9	47.7
Overall intensity variation (%)	-8.2	20.4	-0.2
Scan width, × in (× + 1.05tanθ)^c	0.85	0.85	0.80
# Unique reflections collected	4874	5341	5141
# Observed reflections with $I_{rel} > 2\sigma I_{rel}$	3650	4662	3296
FINAL REFINEMENT PARAMETERS			
Number of variables	286	315	369
R	0.093	0.043	0.077
R_w	0.099	0.044	0.087
g in $w = (\sigma^2(F_0) + g(F_0)^2)^{-1}$	0.008	0.0001	0.1
S (goodness of fit parameter)	1.43	2.50	0.76
Max. shift/e.s.d.	0.011	0.004	0.037
Avg. shift/e.s.d.	0.001	0.000	0.001
Max., min. heights in difference Fourier (eÅ^{-3})	0.64, -0.20	0.19, -0.26	0.34, -0.35

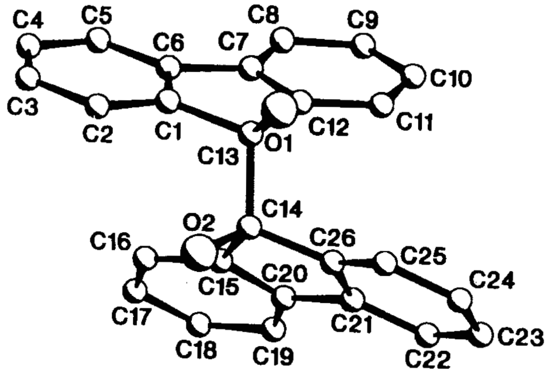

Figure 1 Atom numbering scheme for 9,9'-dihydroxy-9,9'-bifluorene.

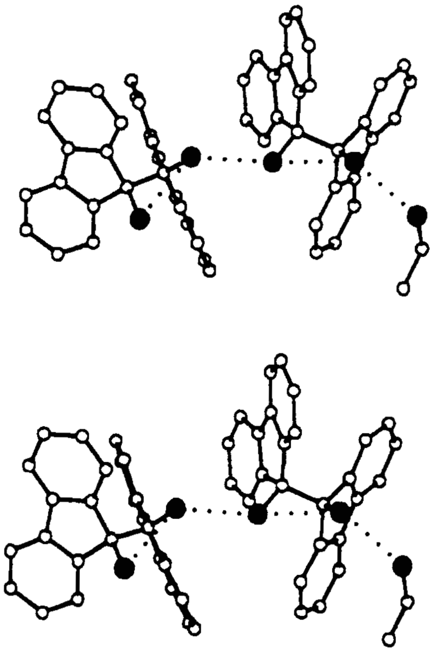

Figure 2 The molecular structure of 2.

host molecule can be described by the torsion angle about the central bond linking the fluorenyl moieties. This angle, O(1)-C(13)-C(14)-O(2) is remarkably constant in all three compounds, varying from 59° to 65°, due to the steric constraints imposed by the bulky fluorenyl groups. The ethanol molecules are situated in cavities, linked by a narrow constriction located at a centre of inversion at Wyckoff position d. These are shown in Fig. 3 which was drawn using the program MOLMAP[9].

For **3**, the positions of all the hydroxyl hydrogens were located unequivocally. This has allowed us to describe the hydrogen bonding scheme in detail as shown in Fig. 4a and 4b. There are five crystallographically unique hydrogen bonds which are shown by dotted lines in Fig. 4a, which link host and guest molecules in double ribbons running along [010]. Details of the hydrogen bonding are given in Table 2. The butanol guest molecules are located in constricted channels which are shown in Fig. 5.

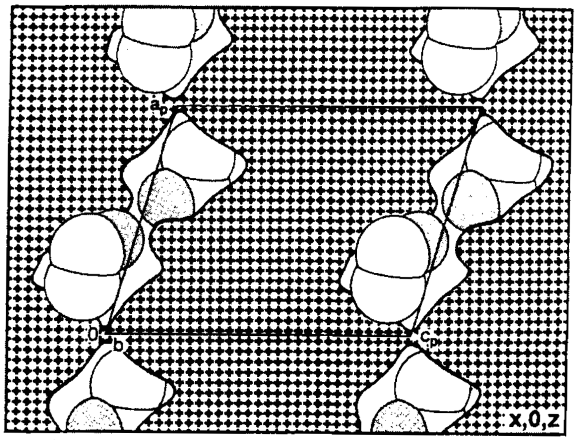

Figure 3 Projected cross-section of the host molecules (hatched area) of **2** on (010) showing the guest molecules (with oxygen atoms shaded) in cavities.

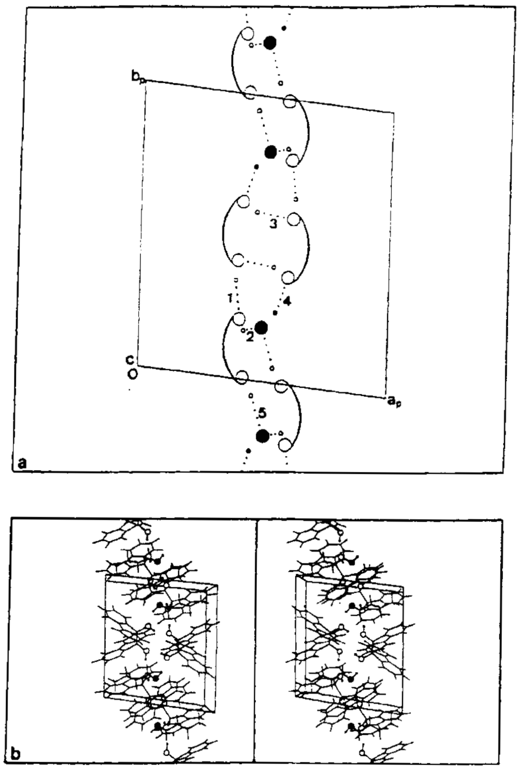

Figure 4 Projections of **3** along [001] showing (a) the oxygen atoms with the unique hydrogen bonds numbered 1 to 5 and (b) the packing between host and guest molecules (the guest atoms are shaded).

In **3**, the crystallographic asymmetric unit comprises two host and two guest molecules. The host molecules are hydrogen bonded into dimers across the diads and form two crystallographically independent columns parallel to [010]. These in turn allow channels to form, into which the pyridine guest molecules are packed and held to the host structures by O-H···N hydrogen bonds. The packing is shown in projection in Fig. 6, while the guest stacking is described in Fig. 7.

Table 2 Details of hydrogen bonding

	Donor	*Acceptor*	*O···O(Å)*	*O···N(Å)*	*O-H(Å)*	*H···O(Å)*	*∠O-H···O(°)*
1	O(1B)	O(2A)	2.727(6)				
	O(2B)	O(2A)	2.771(6)				
	O(2A)	O(1A)	2.775(7)				
	O(1A)	O(1G)	2.715(8)				
2	O(1A)	O(2B)	2.772(2)		0.97(1)	1.83(1)	163(2)
	O(1B)	O(1G)	2.859(2)		0.96(2)	2.04(2)	142(2)
	O(2A)	O(1A)[a]	2.921(2)		0.96(3)	2.01(2)	158(3)
	O(1G)	O(2A)[a]	2.797(2)		0.96(2)	1.91(2)	153(2)
	O(2B)	O(1G)[b]	2.902(2)		0.95(2)	1.96(2)	169(2)
3	O(1A)	N(1G1)		2.69(1)			
	O(2A)	O(1A)	2.753(8)				
	O(1B)	O(2B)	2.765(8)				
	O(2B)	N(1G2)[c]		2.73(1)			
	O(2A)	O(1A)[c]	2.803(7)				
	O(1B)	O(2B)[c]	2.835(8)				

[a] related to donor by -x + 1,-y + 1,-z + 1
[b] related to donor by -x + 1,-y,-z + 1
[c] related to donor by -x + 1/2,y,-z + 1/2
Where H is ommited, hydrogen bonding is inferred by short O···O or O···N contacts

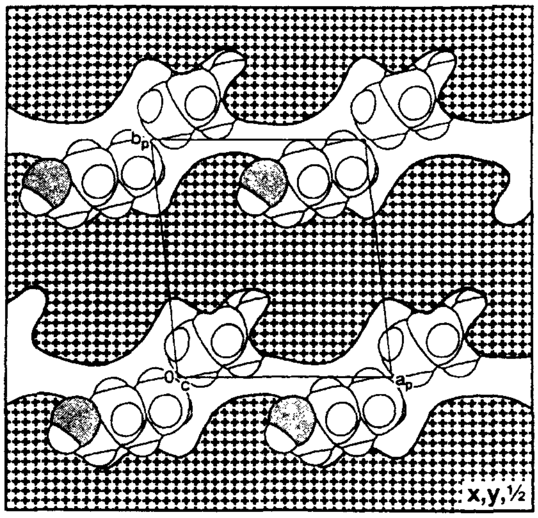

Figure 5 Projected cross-section of the host molecules (hatched area) of **3** on (002) showing the guest molecules (with oxygen atoms shaded) in constricted channels.

The DSC and TG curves are shown in Fig. 8. For each compound, the measured weight loss is in close agreement with the calculated value, confirming the host:guest ratios which were employed in the crystallographic analyses. For each compound there is an endotherm A due to guest loss, followed by a second endotherm B, attributed to the melting of the host compound. The onset temperatures of guest loss and other thermal parameters are listed in Table 3.

The area under the DSC endotherm can, in principle, give the enthalpy change of the guest loss reaction. However these measurements are generally inaccurate because they depend on such factors as heating rates, particle size distribution, flow velocity of the purging gas and the geometry of the calorimeter.

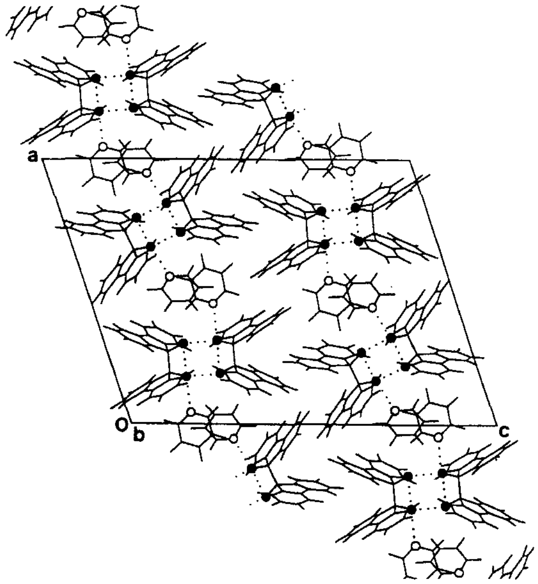

Figure 6 Projection of **4** viewed along [010] with oxygen atoms shaded and hydrogen bonds indicated as dotted lines.

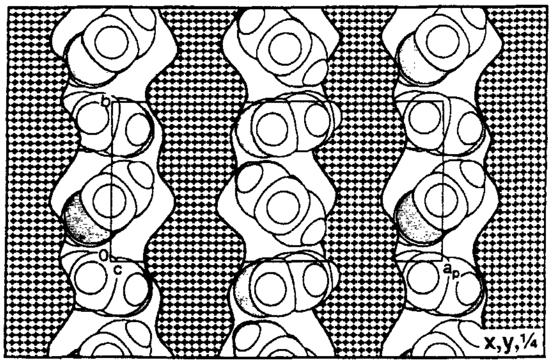

Figure 7 Projected cross-section of the host molecules (hatched area) of **4** on (004) showing the guest molecules in channels parallel to [010].

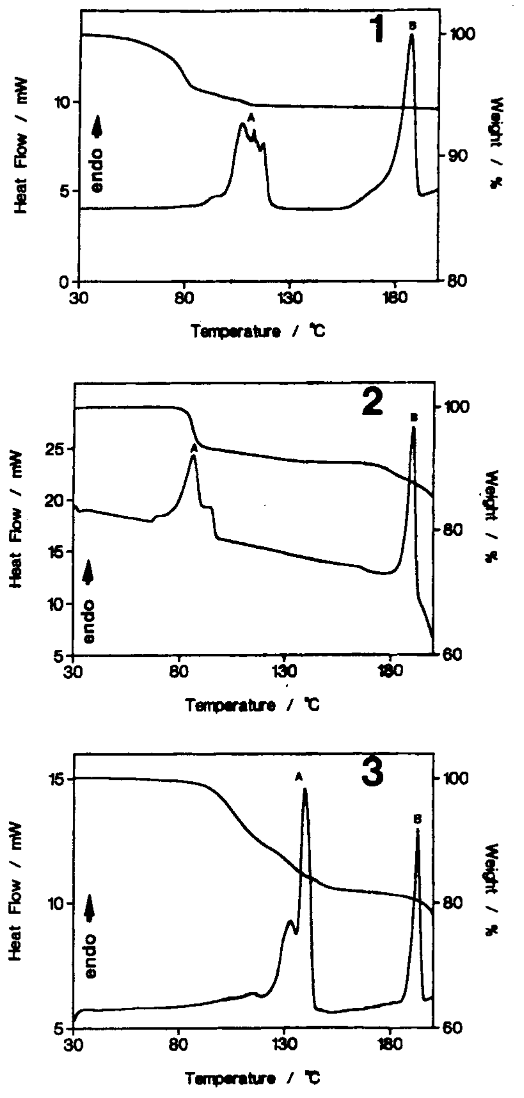

Figure 8 DSC and TG traces of compounds **2** to **4**.

Table 3 Thermal analysis

Compound	*1*	*2*	*3*
Host:guest ratio	2:1	2:1	1:1
Boiling point of guest (°C)	78.5	117.2	115.5
TG			
Calculated weight loss (%)	6.0	9.3	17.9
Measured weight loss (%)	5.9	8.9	17.8
DSC			
Onset temperature of endotherm A (°C)	88	67	120
Onset temperature of endotherm B(°C)	173	180	184

Therefore we have devised a special apparatus which accurately measures the vapour pressure of volatile guests liberated from inclusion compounds. The apparatus consists of a small sample flask (ca.3 cm^3) which can be evacuated and is connected to a pressure transducer. The latter is accurately calibrated to read pressures from 0 to 1 atm. The sample is heated slowly at 0.3 °Cmin^{-1} and the pressure is recorded at various temperatures.

We have carried out this experiment for **2** and obtained the pressure-temperature curve shown in Fig. 9a. The inclusion compound **2** was prepared by dissolving the host in ethanol and evaporating the solution under continuous stirring. This ensured that we obtained the compound as very small crystals, which minimises diffusion barriers of the guest desorption. The curve obtained for the heating process coincides with the one measured on cooling, showing this to be a true equilibrium experiment.

The stoichiometry of the reaction

$$H\cdot{}^{1}\!/_{2}G\ (s,\beta) \rightleftharpoons H(s,\alpha) + {}^{1}\!/_{2}G\ (g)$$

is such that the equilibrium constant $K_e=P^{1/2}$ where P is the vapour pressure of the volatile guest (we have assumed the activity of the volatile guest to be equal to its vapour pressure). The plot of $^1\!/_2 \ln P$ vs $1/T$ is shown in Fig. 9b, and its slope yields a value of $\Delta H = 17.9$ kJmol^{-1} for the guest release reaction.

When an inclusion compound decomposes with loss of guest, this is usually accompanied by a change of phase. We have modified an existing apparatus to measure these phase transitions. This consists of a Weissenberg goniometer which has a stream of hot air blowing on a powdered specimen of the compound under investigation. The specimen is heated at a constant rate and the film cassette movement is coupled to the temperature of the specimen. This allows one to record

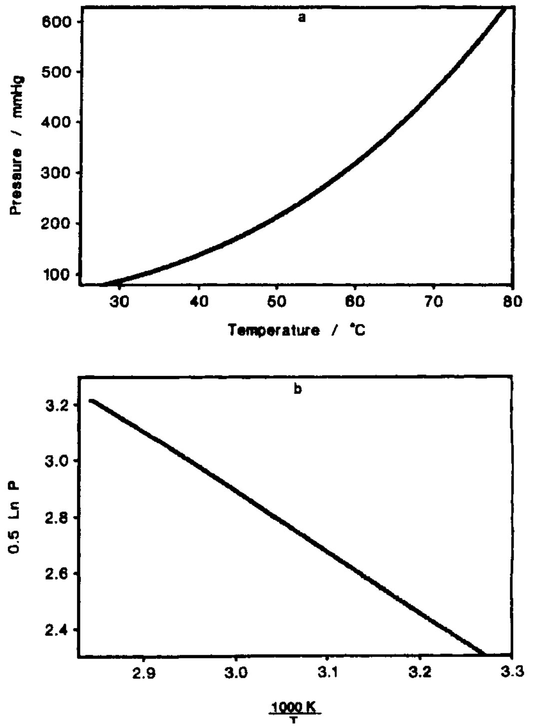

Figure 9 Plots of (a) Pressure vs temperature and (b) 0.5 ln *P* vs 1000/*T* for **2**.

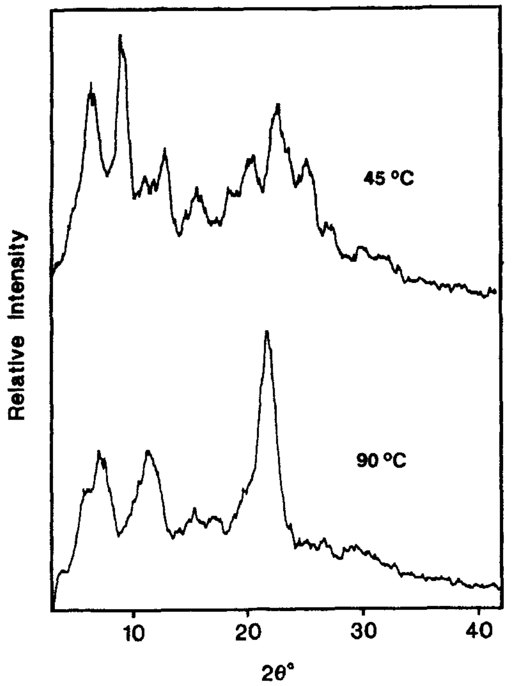

Figure 10 XRD traces of (a) the β-phase of **2** at 45°C and (b) the α-phase at 90°C resulting from thermal decomposition of **2**.

the powder diagram continuously over the selected temperature range and to pinpoint transition temperatures to a precision of about 3°C.

The powder patterns of **2** were recorded continuously from 30 to 115 °C. The initial β-phase of the inclusion compound transforms to the non-porous α-phase at 73°C. Fig. 10 shows the photometer trace of the initial β-phase at 45°C and of the resulting α-phase at 90°C.

This apparatus is similar to that constructed for the analysis of phase transitions of ammonium nitrate,[10] and is proving useful for confirmation of DSC results obtained from the decomposition of clathrates.

REFERENCES

1 Weber, E.; Inclusion Compounds, Vol 4, eds. Atwood, J.L.; Davies, J.E.D. and MacNicol, D.D. Oxford University Press, **1991**, Chapter 5.
2 Bond, D.R.; Nassimbeni, L.R.; Toda, F.; *J. Incl. Phenom. Mol. Recog. in Chem.* **1989**, *7*, 623.
3 Bond, D.R.; Nassimbeni, L.R.; Toda, F.; *J. Cryst. Spectrosc. Res.* **1989**, *19*, 847.
4 Bond, D.R.; Caira, M.R.; Harvey, G.A.; Nassimbeni, L.R.; Toda, F.; *Acta Cryst.* **1990**, *B46*, 771.
5 Bourne, S.A.; Nassimbeni, L.R.; Toda, F.; *J. Chem. Soc., Perkin Trans. 2*, **1991**, 1335.
6 Nassimbeni, L.R.; Johnson, L.; Toda, F.; *Supramol. Chem.* **1993**, 2, 233.
7 Barbour, L.J.; Bourne, S.A.; Caira, M.R.; Nassimbeni, L.R.; Weber, E.; Skobridis, K.; Wierig, A.; *Supramol. Chem.* **1993**, *1*, 331.
8 Gomberg, M.; Bachmann, W.E.; *J. Am. Chem. Soc.* **1927**, *49*, 236.
9 MOLMAP, Barbour, L.J.; unpublished computer program, **1993**.
10 Boeyens, J.C.A.; Ferg, E.; Levendis, D.C.; Schöning, R.R.L.; *S. Afr. J. Chem.* **1991**, *44*, 42.